Black Sea Journal of Engineering and Science
doi: 10.34248/bsengineering.1530795

Open Access Journal
e-ISSN: 2619 – 8991

Research Article
Volume 7 - Issue 5: 1007-1013 / September 2024

DESIGN A COMPUTER CONTROLLED UNMANNED UNDERWATER VEHICLE THRUSTER USING SMART CLOSED LOOP CONTROLLER

Ihab ELAFF[1]*

[1]*Üsküdar University, Faculty of Engineering and Natural Sciences, Department of Computer Engineering, 34662, İstanbul, Türkiye*

Abstract: The first step of designing an Unmanned Underwater Vehicle (UUV) depends mainly on the selection of the thrusters, as UUVs require many thrusters to be installed onboard for smooth operation. The problems with the widely used thrusters in UUVs are the relatively large dimensions, and they just spin in the water without reporting any kind of important information such as the status of the thruster and the RPM of the motor. This project aims to design and implement a new computer-controlled thrusting system from end-to-end that fits various UUVs with more advantages including a smaller sized thruster, cheaper in price, and with more additional smart capabilities that report the thruster's instantaneous RPM, power consumption, proper operation, malfunctions, damages, and water stream blockage. The new thruster has Forward Thrust of 3.5 kgf, Reverse Thrust of 2.45kgf, and a maximum Power consumption 172.8 which is close to other widely used thrusters with the advantage of reporting operational status.

Keywords: Thruster, ETR100, UUV, Blue robotics, SeaBotix

***Corresponding author:** Üsküdar University, Faculty of Engineering and Natural Sciences, Department of Computer Engineering, , 34662, İstanbul, Türkiye
E mail: ihab.elaff@uskudar.edu.tr (I. ELAFF)
Ihab ELAFF https://orcid.org/0000-0002-0913-5476

Received: August 09, 2024
Accepted: September 06, 2024
Published: September 15, 2024

Cite as: Elaff I. 2024. Design a computer controlled unmanned underwater vehicle thruster using smart closed loop controller. BSJ Eng Sci, 7(5): 1007-1013.

1. Introduction

The discovery of the underwater world presents a big challenge to human limitations. Exploration of the underwater environment of the deep oceans is handled nowadays with Unmanned Underwater Vehicle (UUV) (Prasad and Sai Kiran, 2020). UUVs such as Remotely Operated Vehicle (ROV) (Capocci et al., 2017) and Autonomous Underwater Vehicle (AUV) (Sánchez et al., 2020) have recently become a promising growing field in the underwater environment exploration industry. Exploration includes: sea-floor reconstruction (Song et al., 2020), underwater life exploration (Macreadie et al., 2018), shipwreck exploration (Patterson et al., 2012), underwater-pipelines inspection (Ho et al., 2020), oil and gas exploration (Khojasteh and Kamali, 2017) etc. All those applications don't require fast motion and large torque. However, they require many thrusters for fine-motion control and low power consumption, while also small size is an important issues to be considered. Brushed DC motor such as SeaBotix BTD150 thrusters (Seabotix BTD150, 2024) or brushless DC motor such as Blue Robotics T200 thrusters (Blue Robotics, T200, 2024), and SAAB Seaeye thrusters (SAAB Seaeye, 2024) are widely used by many UUVs. Selection of suitable thruster for certain applications affects the whole design of the UUV. For motion control, UUV's designers usually support 4 to 8 thrusters at the corners with a titled angle on a plan inside or outside the UUV to obtain a smooth control of planner motion and 2 to 4 thrusters perpendicular to this plan for vertical motion. This relatively large number of thrusters affects the UUV body design and workspace, where thrusters with relatively large length will make its placement in the UUV somehow more difficult than the shorter length. Then, selection of the thruster is a critical aspect in designing the UUV body.

One important factor during UUV motion control is specifying the thrust of each thruster instantly to follow the desired trajectory. Thrust can be determined based on the motor's RPM, the parameters of the thruster's propeller and the water parameters. Measurement of the RPM in the widely used thrusters such as T200 and BTD150 is not present as an option. Doing that using a tachometer or an IR counter requires additional hardware to be installed on the thruster's body which will cause more drag and requires some additional wiring and caution to fit the underwater environment. Another important factor during UUV operation is power consumption, especially in AUVs. This requires measuring the current consumption in each thruster. This also is not present as a built-in option in the widely used thrusters. Knowing the RPM and the current of each thruster will help in evaluating the status of the system components and the working environment.

This project aims to design and implement a computer-controlled thrusting system from end-to-end that fits

various UUVs with more advantages including, smaller than existing thrusters, cheaper in price, and with more additional smart capabilities that report thruster's instantaneous RPM, power consumption, proper operation, malfunctions, damages, and water stream blockage.

2. Materials and Methods

The development process of the new thrusting system is divided into 4 layers (Figure 1): physical layer, mechanical layer, electrical/electronic layer and computer layer.

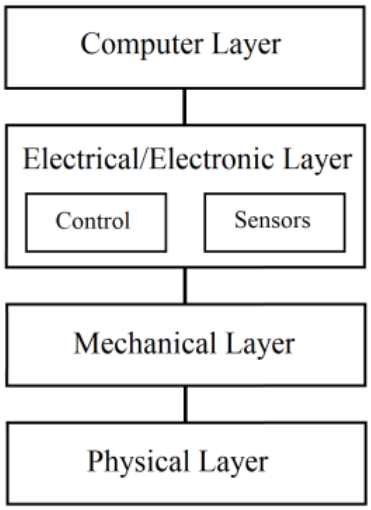

Figure 1. Thrusting system layers.

2.1 Physical Layer

Thruster is physically divided into 2 parts, the propeller and the casing. During thruster design, some issues have been taken into consideration, such as reliability, maintainability, usability, produceability, and affordability, scope of applications, targeted thrust, size of the thruster, number of propeller blades and safety.

For UUVs body design, the smaller the size of the thruster, the better to fit in the vehicle. Referring to the widely used thrusters such as BTD150 and T200, 100 mm outer diameter of the new thruster ETR100 has been selected as a starting point. Blue-Robotics and SeaBotix thrusters have relatively long motor casing extended outside the thruster head which adds some physical limitations to UUV design. In ERT100 thruster, it was taken into consideration to embed the motor inside the thruster casing saves a lot of space compared to other thrusters.

The propeller and the thruster casing have been designed using OpenProp (2024) which is used for design and analysis of marine propellers and horizontal-axis turbines. OpenProp can run on MATLAB or Octave (Epps, 2016; Epps and Kimball, 2013; OpenProp, 2024).

The number of blades and hub diameter are related to the required thrust and motor parameters (RPM, Current and Voltage). As selection of those design parameters is a recursive process, many trials with different parameters have been tested until suitable values have been selected. EMAX CF2822 (2024) brushless motor is selected in the design, where the 2 blades propeller with 20 mm hub diameter has been selected to obtain a thrust of 4 kgf (Figure 2).

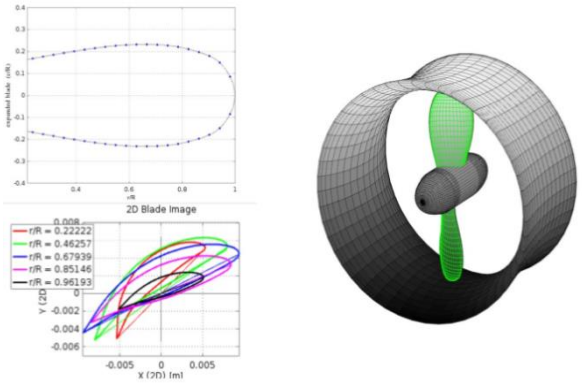

Figure 2. OpenProp design of ETR100 thruster

The generated blade profiles have been exported and reconstructed using FreeCAD (GNU) as 3D object (Figure 3). The hub has been split into 3 parts, namely: front nozzle, cylinder, and rear nozzle. To embed the motor inside the propeller's hub, the cylinder part of the hub has been modified to a frustum of 35 mm base diameter and 20 mm top diameter. An additional cylinder is added to the base of the frustum to cover the rest of the motor body which did not affect the forward thrust too much.

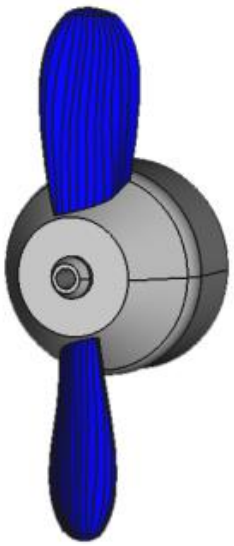

Figure 3. 3D model of ETR100 propeller.

The ETR100 thruster's casing is designed as a tube with front and rear supports to fix the motor in the center of that tube using 8 flat beams. Protection nets on both sides have been extended as edgy-rings through those flat beams (Figure 4). The inner profile of the thruster takes the same convex profile of the generated design from the OpenProp (Figure 2). However, the outer profile of the thruster is chosen to have a straight profile for alignment purposes on UUVs bodies. The front support takes the same profile of the 20mm propeller's hub's

nozzle; however, the rear support has been designed as a frustum of 35mm base diameter and 32 mm top diameter to hold the motor's base. Finally, the design has been realized using a 3D printer (PLA material) for testing and evaluation (Figure 5).

Figure 4. ETR100 front (top) and back (bottom) casing design.

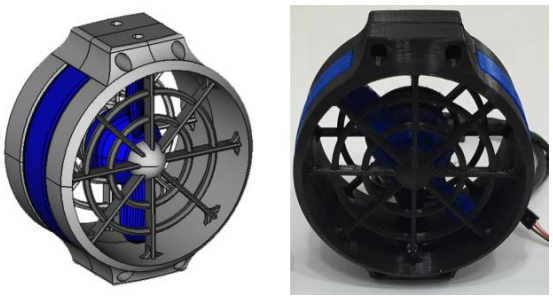

Figure 5. 3D model of ETR100 thruster (left) and 3D printed model (right).

2.2 Mechanical Layer

The main issue of the mechanical layer is to select a suitable motor for running the propeller inside the casing in a smooth and stable operation. Among different types of motor, a brushless motor has been selected because it is compact in size, light in weight, relatively low cost, run using DC supply at low voltage, provide good torque and speed without any gearbox, suitable for use in underwater environment directly without special sealing, and it can resist water pressure at large depths without special preparations. It should be noticed that the water density is much larger than air, which makes the propeller subjected to more reverse torque that will slow down motor rotation and implies the propeller slips if it is not supported properly on the motor's rotor. Because of that, among different brands of brushless motors, EMAX CF2822 has been selected because, in addition to the above advantages of brushless motors, its rotor part has 3 metallic shoulders which are used to rotate the propeller without slipping and without any additional support (reliability and produceability). It was sufficient to support the motor base using 4 nipples placed in the floor of the frustum of the back cover without any screws. For stable operation, the tip of the rotor's axe is placed inside a bearing which is located in the cavity of the front cover's nozzle (Figure 6).

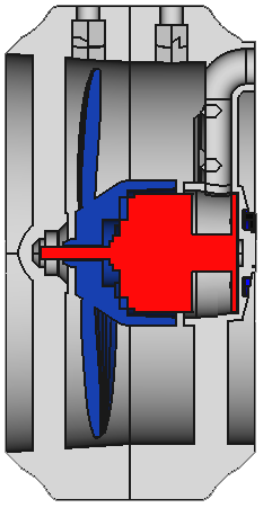

Figure 6. ETR100 thruster cross-sectional view showing inner casing profile and motor placement.

2.2 Electrical and Electronic Layer

The brushless motor is derived using Electronic Speed Controller (ESC) (Gorospe et al., 2017). In simple words, ESC is composed of a microcontroller, some MOSFETs pairs and a zero-crossing circuit. Each MOSFET pair is usually composed of P-MOS and N-MOS connected in series. Each wire of brushless motor is connected to an attachment point between the two MOSFETs. The MOSFET pair is responsible for connecting any motor's wire either to the supply's voltage or to the supply's ground. Such as any brushless motor, the motor will step according to a switching sequence of the MOSFET pairs. The MOSFET pairs sequencing operation is controlled by the ESC's microcontroller according to a Pulse Width Modulation (PWM) input signal from the deriving UUV controller. ESC is capable of measuring the completion of the mechanical action corresponding to a certain sequence by measuring the Back EMF (BEMF) of the free wire using a built-in zero-crossing measurement circuit. A complete rotation of the motor's rotor will be achieved after the zero-crossing circuit triggers a number of times equal to the number of the motor's poles.

Measuring the RPM of the motor while it is running will reflect the corresponding thrust of the propeller. Also, the ability to measure both the motor's RPM and its current consumption is useful in determining the rate of power consumption and the status of the thruster and ESC in case of any malfunctions or improper operating conditions such as blockage of the water stream or operation in the air that require halting the motor or intervention from the controller.

Measurement of the RPM under the water using a tachometer or an IR counter requires additional hardware to be installed on the thruster's body which will cause more drag and requires some additional

wiring and caution.

Developing an entire ESC that exporting sensor values is an unnecessary job because updating existing brands would be much easier and much more cost-effective. By adding an external zero-crossing measurement circuit to the ESC wires, the motor's RPM can be determined by the UUV controller from inside the air chamber without connecting extra components to the thruster itself. The EMAX CF2822 contains 12 poles which make one revolution being achieved after 12 triggers from the zero-crossing circuit. The following circuit (Figure 7) is capable of monitoring both the current consumed by the thruster and the zero-crossing pulsation. Also, combining readings from the RPM and the current will help to identify the status of the motor, the ESC and the working environment as stated earlier.

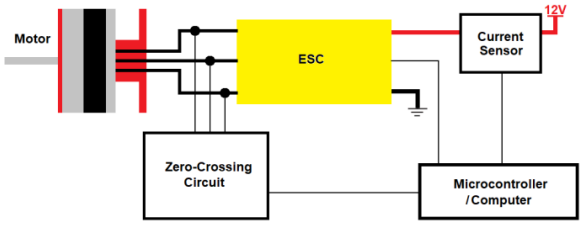

Figure 7. Circuit diagram of the motor's rotation position monitoring and current consumption monitoring

2.3 Computer Layer

The computer layer is concerned with 2 parts: the firmware of the ESC's microcontroller and the code in the UUV controller. The majority of ESC brands in the market derive the motor in one direction and very few brands work in both directions, where this depends on the firmware ability to shift MOSFET switching in both directions. There are two open-source firmware which can replace the original firmware of many ESC brands for a better, smoother and customizable operation; namely: SimonK (SimonK, 2024) (used by Blue Robotics' ESC deriver after some few updates) and BLHeli (2024). However, those firmwares are designed to work with drones that function according to air parameters. Using the ESC for the underwater environment requires some modifications for a slower response.

SimonK firmware has been used to re-program Hobbyking ESC20 (2024) for deriving the ETR100 thruster. Some updates have been done to the original SimonK firmware including: enabling to rotate the motor in both directions, adjusting the PWM input range between 1120 and 1865 uSec for controlling the ESC's output current (selection of those values will be discussed in results), adjusting dead band to be between 1450 uSec to 1550 uSec to avoid undesirable motor movement due to heating of the built-in crystal oscillator of the ESC's microcontroller during use, adjust initializing pulse to be at 1500 uSec, , limit the maximum throttle jump to try to prevent overcurrent, remove unnecessary beeps and disable error code of no operation for long time. The updated SimonK firmware is used instead of the original firmware of the Hobbyking ESC20.

Violating the synchronization between mechanical action and electronic sequence causes SimonK firmware to halt the motor. So, reaching the desired RPM quickly in the underwater environment is not applicable to the original setting of SimonK firmware. Modifying the timeouts of the SimonK code was not successful after many trials. However, with the help of the external zero-crossing circuit, setting the suitable PWM for building-up to the required RPM could be achieved by monitoring the delay between each 2 successive pulses, which is in the case of the used components and water conditions is 397 uSec in the average at the maximum PWM. This will make the thruster operates with the maximum of 1048 RPM.

The current monitoring module combined with the RPM at any PWM input can indicate different conditions of the system according to the following table (Table 1), so the UUV controller can take proper actions for each case.

Referring to that table, the UUV controller could be programmed to take action by sending a warning to the user or disable the motor from running for a long time to protect the motor from possible damage.

Table 1. Thrusting system status

RPM Range	Current Range	Possible Problems
Normal	Normal	• No problems
Normal	Low	• thruster is still in the air • blades of the propeller are broken • The shaft of the motor is not connected to the propeller
0 or very low	0	• The ESC is damaged • Wire (s) of the motor not connected to ESC. • the power supply is low or not connected
Normal	High	• The propeller or the motor is jammed. • blockage in the inlet or the outlet of the thruster • fluid that surround the thruster is of higher viscosity (such as oil)
0 or very low	High	• Motor motion is blocked • Short circuit inside the ESC

3. Results

The thrust profile is generated by running the ETR100 thruster in sweet water in the room temperature using 12 VDC power supply and PWM timing adjusted (initially) to operate from 1100 uSec to 1900 uSec. The

dead band has been adjusted at the beginning between 1450 and 1550 uSec is used as stop state, the timing band between 1550 and 1900 uSec is used for forward thrust and the timing band between 1100 and 1450 uSec is used for reverse thrust. Motor is initialized by sending PWM signal of 1500 uSec for a few seconds.

For thrust measurement, a mechanism has been developed as a class-I lever system where the thruster is placed on the tip of one side of the lever and the electronic mass scale on the other tip. The fulcrum of the lever has been supported at the top side of a water tank where the thruster is immersed entirely at a suitable height away from the tank floor and the electronic mass scale has been supported from its other side on a fixed reference point above the fulcrum.

Finally, the thrust profile and current profile have been created by measuring the thrust and the current consumption (Table 2) of the ETR100 during running at different PWM inputs from an external microcontroller many times and an average reading has been taken (Figure 8 and Figure 9).

Table 2. Measurements of the current and the thrust of ETR100 at different PWM

PWM (uSec)	Current (Amp.)	Thrust (kgf)
1100	17.72	-2.70
1150	13.66	-2.35
1200	9.96	-2.13
1250	6.52	-1.57
1300	3.72	-1.15
1350	1.63	-0.74
1400	0.43	-0.49
1450	0	0
1500	0	0
1550	0	0
1600	0.68	1.20
1650	2.18	1.7
1700	4.46	2.55
1750	7.48	3.14
1800	10.98	3.36
1850	14.77	3.53
1900	18.85	3.63

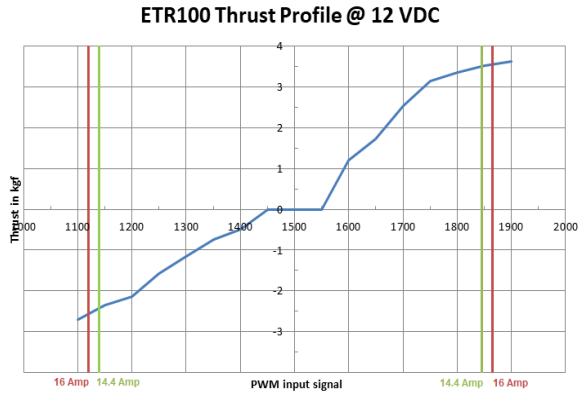

Figure 8. Thrust profile of ETR100 thruster.

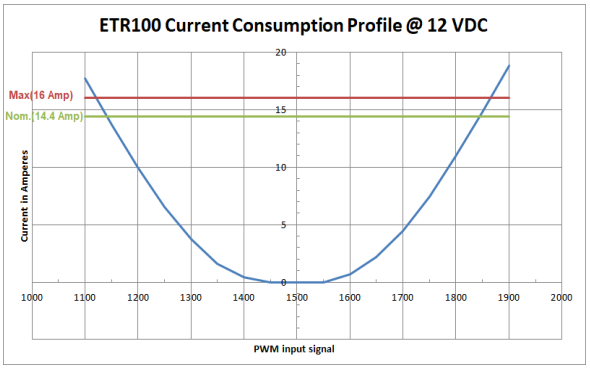

Figure 9. Current consumption profile of ETR100 thruster.

To control the maximum current that can be obtained from the ESC to derive the motor, the firmware of the ESC has been updated to truncate any input PWM signal outside the band 1120 and 1865 uSec. This truncation allows the ESC to supply up to 16 amperes, which is the maximum current of the EMAX CF2822; however, for long term operation of the thruster, the recommended maximum operating current is 14.4 Amps (10% lower than the maximum allowed current).

While the above testing is based on sweet water in the room temperature conditions, it is not the case when the UUV operates in seawater at different temperatures and with water stream currents flowing in unpredictable directions. So, determining the RPM using the external zero-crossing circuit would give a more accurate figure of the real generated thrust.

4. Discussion and Conclusion

A new thrusting system for UUVs has been developed to overcome some of the disadvantages of the other widely used brands and is equipped with smart capabilities. It is composed of the newly designed ETR100 thruster of compact size, regular ESC with modified firmware and additional modules to measure the current and the revolution speed of the motor. This system provides suitable thrust for exploration applications at standard 12 VDC supply and because of its smaller size compared to other thrusters (Figure 10) it will be much comfortable during the design of the UUV.

By comparing ETR100 to T200 and BTD150 (Table 3), ETR100 has a better advantage in size over the other 2 thrusters. For nominal operation, ETR100 is set to work at 90% of its maximum current (14.4 amperes). T200 produces more thrust for its nominal operation compared to ETR100; however, it consumes more power which causes the ESC to have higher temperature buildup during operation. Furthermore, BTD150 compared to ETR100, has lower thrusts and also lower power consumption, which makes ETR100 the middle performance between both thrusters. It is possible to run T200 thruster with up to 20 volts which produce more thrust and this is an advantage over the ETR100.

Because of the high current consumption of a brushless

motor, its temperature gets higher during the operation, which will cause the coil resistance to rise and affect motor performance. However, using the brushless motor underwater will make the surrounding water reduce motor temperature, which will keep the motor at high performance all the time.

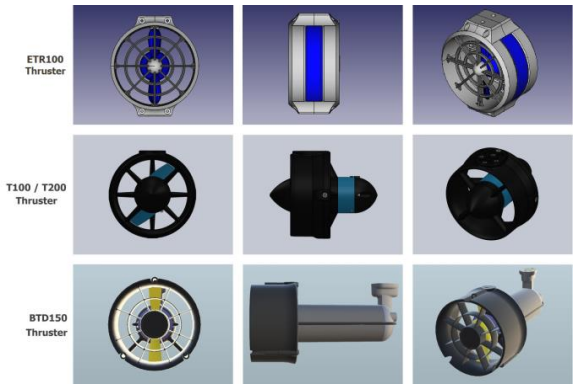

Figure 10. Comparison between ETR100, T100/T200 and BTD150 sizes.

Table 3. Comparison between ETR100, T200 and BTD150 performance parameters

Parameter	ETR100	T200	BTD150
Dimensions (mm)	D100 x 60	D100 x 113	D95 x 171
Motor Type	Brushless	Brushless	Brushed
Propeller Blades	2	3	2
Forward Thrust	3.5 kgf	3.71 kgf(@12V)	2.2 kgf
Reverse Thrust	2.45kgf	2.92 kgf(@12V)	-
Power in Watts	172.8	204 (@12V)	81
Operating Voltages	12 VDC	12, 16, 20 VDC	19.1 VDC
Current in Amp.	14.4	17	4.25

Developing a native firmware for ESC that works with water parameters is a very complicated task as many parameters and routines should be considered. It was much easier to adjust some settings in the ESC's firmware and complete the rest of tasks at computer layer level.

For realizing how a thruster's body causes a drag, a CFD simulation using OpenFOAM (2024) is used to generate surface pressure profiles for ETR100 and the other thrusters. All thrusters have been inserted inside a tube of 1000 mm in diameter and 2000 mm in length. Water flow in the tube was fixed at a magnitude of 10000 mm/sec (Figure 11). Then pressure drag is generated by the resolved components of the forces due to pressure acting normally on the surface at all points. It is computed using ParaView (2024) utility as the integral of the flow direction component of the pressure forces acting on all points on the body.

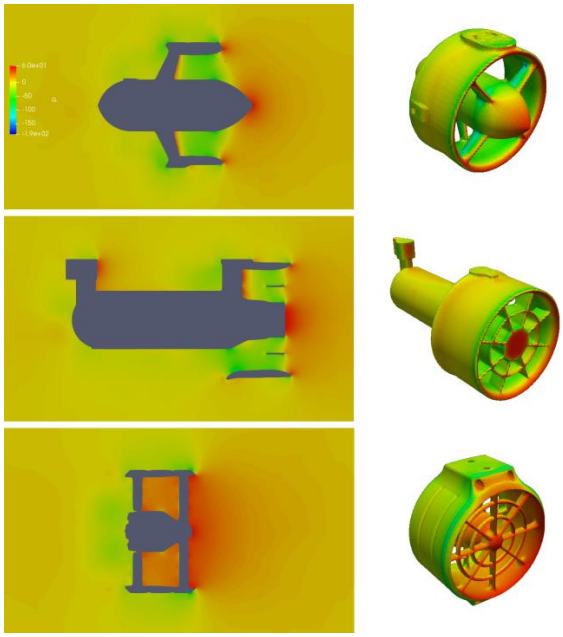

Figure 11. CDF simulation of pressure force for some thrusters (from the top) T200, BTD150 and ETR100.

Simulation results show that ETR100, T200 and BTD150 bodies give drag force -0.22N (-0.0223 kgf), -0.14N (-0.0138 kgf) and -0.15N (-0.0154 kgf) respectively. Even though ETR100 body gives relatively the highest drag, the worst case loss in thrust is extremely very low (0.64%) compared to the benefits of the safety network and the symmetric body design. As future work, more improvements to the thruster's body will be applied to reduce drag as well as use more blades for the propeller to improve efficiency.

Author Contributions

The percentages of the author contributions are presented below. The author reviewed and approved the final version of the manuscript.

	I.E.
C	100
D	100
S	100
DCP	100
DAI	100
L	100
W	100
CR	100
SR	100
PM	100
FA	100

C=Concept, D= design, S= supervision, DCP= data collection and/or processing, DAI= data analysis and/or interpretation, L= literature search, W= writing, CR= critical review, SR= submission and revision, PM= project management, FA= funding acquisition.

Conflict of Interest

The author declared that there is no conflict of interest.

Ethical Consideration

Ethics committee approval was not required for this study because of there was no study on animals or humans.

Acknowledgements

This work is supported by TUBITAK TEYDEP 1507, Project No.: 7150974, Project Title: EngTechs Underwater Vehicles Thruster (UVT): End-to-End Computer Controlled Thrusting System Design and Implementation.

References

BLHeli. 2024. Firmware page. URL: https://github.com/bitdump/BLHeli. (accessed date: 9 August 2024).

Blue Robotics T200. 2024. Thruster specifications. URL: https://bluerobotics.com/store/thrusters/t100-t200-thrusters/t200-thruster-r2-rp/ (accessed date: 9 March 2024).

Capocci R, Dooly G, Omerdić E, Coleman J, Newe T. 2017. Inspection-class remotely operated vehicles—a review. J Marine Sci Engin, 5(1): 13.

EMAX CF2822. 2024. Brushless motor specifications. URL: https://emaxmodel.com/products/emax-cf2822-1200kv-brushless-motor-for-rc-airplane-multicopter (accessed date: 9 March 2024).

Epps B. 2016. On the rotor lifting line wake model. J Ship Prod Design, 32(3): 31-45.

Epps B, Kimball R. 2013. Unified rotor lifting line theory. J Ship Res, 57(4):181-201.

Gorospe G, Kulkarni C, Hogge E, Hsu A, Ownby N. A study of the degradation of electronic speed controllers for brushless DC motors. URL: https://ntrs.nasa.gov/api/citations/20200000579/downloads/20200000579.pdf (accessed date: 9 March 2024).

Ho M, El-Borgi S, Patil D, Song G. 2020. Inspection and monitoring systems subsea pipelines: A review paper. Struct Health Monitor, 19(2): 606-645.

Hobbyking ESC 20. 2024. Amperes specifications. URL: https://hobbyking.com/en_us/hobbyking-20a-2-4s-esc-3a-ubec.html?___store=en_us (accessed date: 9 March 2024).

Khojasteh D, Kamali R. 2017. Design and dynamic study of a ROV with application to oil and gas industries of Persian Gulf. Ocean Engin, 136: 18-30.

Macreadie P, McLean D, Thomson P, Partridge J, Jones D. 2018. Eyes in the sea: Unlocking the mysteries of the ocean using industrial, remotely operated vehicles (ROVs). Sci Total Environ, 634: 1077-1091.

OpenFOAM. 2024. URL:https://www.openfoam.com/ (accessed date: 9 March 2024).

OpenProp Software v3.3.4. 2024. Open-source software for the design and analysis of marine propellers and horizontal-axis turbines (2013). URL: https://www.epps.com/openprop. (accessed date: 9 March 2024).

ParaView. 2024. URL:https://www.paraview.org/ (accessed date: 9 March 2024).

Patterson M, Elliott J, Niebuhr D. 2012. A STEM experiment in informal science education: ROVs and AUVs survey shipwrecks from the American Revolution. Oceans, 2012: 1-8.

Prasad MPR, Sai Kiran P. 2020. Development of deep sea unmanned underwater robots: a survey. In: IEEE 17th India Council International Conference (INDICON); 10-13 December, New Delhi, India; pp: 1-7.

SAAB. 2024. Seaeye thrusters specifications. URL: https://www.saabseaeye.com/uploads/thrusters-group-datasheet-rev6.pdf. (accessed date: 9 March 2024).

Sánchez PJB, Papaelias M, Márquez FPG. 2020. Autonomous underwater vehicles: Instrumentation and measurements. IEEE Instrument Measure Magazine, 23(2): 105-114.

Seabotix BTD150. 2024. Thruster specifications. URL: http://ocean-innovations.net/OceanInnovationsNEW/SeaBotix/BTD150_Data_Sheet.pdf. (accessed date: 9 March 2024).

SimonK. 2024. Firmware page. URL: https://github.com/sim-/tgy. (accessed date: 9 March 2024).

Song Y, Choi S. 2020. Underwater 3D reconstruction for underwater construction robot based on 2D multibeam imaging sonar. J Ocean Engin Technol, 30(3): 227-233.